Modeling Polymer Degradation by Atomic Oxygen in Low Mars and Earth Orbits: Are Diffuse Functions Necessary?

Dario Campisi[1(✉)], Giacomo Pannacci[2], Nadia Balucani[2], and Marzio Rosi[3,4]

[1] Engineering Department, University of Perugia, via Duranti 93, 06125 Perugia, Italy
dario.campisi@unipg.it, darcampisi@outlook.com
[2] Department of Chemistry, Biology and Biotechnology, University of Perugia, via dell' Elce di Sotto 8, 06123 Perugia, Italy
[3] Department of Civil and Environmental Engineering, University of Perugia, via Duranti, 93, 06125 Perugia, Italy
[4] Istituto CNR di Scienze e Tecnologie Chimiche "Giulio Natta" (CNR-SCITEC), via dell' Elce di Sotto 8, 06123 Perugia, Italy

Abstract. Materials used in satellites, often composed of organic polymers, are subject to degradation by highly reactive atomic oxygen in low Earth and Mars orbits. The local structures of these polymers often feature fused aromatic rings, resembling small polycyclic aromatic hydrocarbons (PAHs). Computational chemistry calculations, such as density functional theory (DFT), provide a method for estimating the chemical resistance of these moieties. The choice of basis sets in DFT calculations is a critical factor in accurately describing the molecular electronic density in the fragmentation pathways of PAH degradation. In particular, the inclusion of diffuse functions in the basis set is necessary for capturing long-range interactions and charge transfer effects. However, when modeling PAHs, computational limitations become a challenge.

Here, we assess the accuracy of Pople basis sets, polarization-consistent contracted basis sets (pcseg-n), and correlation-consistent basis sets (cc-pVnZ) using the established ωB97X-D3BJ long-range DFT functional. Additionally, we evaluate the impact of including diffuse functions on the performance of the calculations in terms of energy accuracy and computational cost. These basis sets were tested on two PAH samples, naphthalene and phenanthrene. We found that diffuse functions do not significantly affect the performance of the ωB97X-D3BJ functional, and that cc-pVTZ provides the best balance of accuracy and computational efficiency.

Keywords: Basis Sets · DFT · Polymers

© The Author(s), under exclusive license to Springer Nature Switzerland AG 2026
O. Gervasi et al. (Eds.): ICCSA 2025 Workshops, LNCS 15888, pp. 272–288, 2026.
https://doi.org/10.1007/978-3-031-97596-7_18

1 Introduction

The interaction of atomic oxygen O(^{3}P) with polymers (Fig. 1) is a key factor in determining the durability of materials used in satellite missions, particularly in low Earth orbit (LEO) and low Mars orbit (LMO), that extend up to 2000 km above the planets. Due to the high reactivity of atomic O in these environments, polymeric surfaces of satellites undergo significant erosion, necessitating a fundamental understanding of the underlying chemical processes. [1]

Aerospace applications frequently rely on polymeric films, advanced composites, and thermoplastic materials due to their insulation, low weight and high flexibility. Exposure of these materials to LEO and LMO conditions, which are highly oxidative environments, causes polymer erosion, significantly reducing their durability and functional effectiveness over time. However, the erosion rate of polymers varies, as it depends on their physical and chemical properties, which, in turn, are influenced by the polymer's electronic structure. [2] The LEO exposition of 40 different polymers and graphite, including those used in space missions and polymers with various chemical structures for different applications, has resulted in the development of a database of erosion rates. [3] These experiments have shown that polymers capable of enduring decades of exposure to O(^{3}P) quickly degrade and break down into CO or other volatile molecules. To protect them, polymers are now shielded by coatings made of materials resistant to degradation by atomic O(^{3}P). However, imperfections in the coating, either from the deposition process or physical damage occurring during orbit, cause erosion of the polymer substrates. Even though self-healing polymers have been developed, they still have an Achilles' heel, as their structural chains might have weak bonds that can be broken by O. [4]

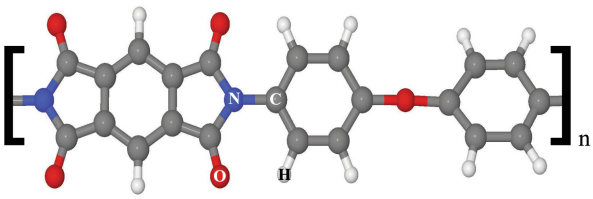

Fig. 1. Example of a polymer material used in satellites: Kapton (poly-oxydiphenylene-pyromellitimide) molecular unit (n > 1). Atomic labels are provided for selected atoms and correspond to all atoms of the same color category.

Despite the availability of ground-based simulation and exposure data, the reaction mechanism at the microscopic level remains obscure. Given the complexity of the systems, theoretical studies remained confined to molecular dynamics simulations [5–7] that, however, did not treat important aspects that strongly affect O reactions with organic compounds like intersystem crossing (ISC) to

the underlying singlet potential energy surface. Previous combined experimental and theoretical work from our laboratory on the bimolecular reactions of atomic oxygen with organic compounds, including several aromatics, demonstrated that the extent of ISC strongly depends on the characteristics of the triplet and singlet PESs and their coupling terms. [8–19] To further explore this, we have initiated a systematic investigation of the reactions between atomic oxygen and aromatic compounds bearing different functional groups that mimic the local structure of space polymers. By integrating experimental data with theoretical calculations of the adiabatic singlet and triplet PESs, as well as product branching fractions, we aim to quantitatively estimate the extent of ISC in a semi-empirical manner, thereby alleviating the challenges associated with a rigorous theoretical treatment of ISC. This will, in turn, allow us to identify the most vulnerable moieties in the polymer skeleton.

Density functional theory (DFT), a quantum chemistry methodology, has been employed to characterize the PES of the O atom reacting with organic molecules due to its computational feasibility. [20] DFT is the ground for characterizing the main intermediates and barriers, which are then used in conjunction with higher-level post-Hartree-Fock (post-HF) methodologies (e.g., CCSD(T) and CASPT2 methods) to compute more accurate energies. [8] However, post-Hartree-Fock methods are feasible for molecular species with fewer than 10 atoms. [21] The problem arises when larger molecular species need to be considered, such as polycyclic aromatic hydrocarbons (PAHs). [22] Nevertheless, for studies based on cross-beam experiments, branching fractions are required to derive the mechanism. These fractions are not sensitive to the exact value of the barriers but rather to the relative variation in energy. [9,23,24]

PAHs are also of interest because they are ubiquitous in interstellar space [25,26] and planetary systems [27–29] due to their easy formation in combustion processes or processes akin to sooting flames in interstellar space. [22,30,31] They are highly resistant to destruction because of their large bond energies, which prevent degradation. [29] However, due to their large structure, post-HF methods are not feasible. Therefore, understanding the accuracy of DFT methodologies is needed to accurately reproduce experimental data. [20] DFT methodologies rely on the accuracy of two important factors: the exchange-correlation (XC) functionals and the basis sets. XC functionals are dependent on specific factors, and several types have been developed over the years to reproduce properties of interest. [22,32] In the case of O-attack on aromatic molecules, the range-separated ωB97X exchange-correlation functional, [33] in conjunction with the Grimme dispersion correction, [34] has been shown to accurately reproduce the PES of O reacting with several organic molecules for both the triplet and singlet states, compared to experiments. [13,14,17,20,35]

Another critical aspect of such calculations is the choice of basis sets, which define the level of accuracy in representing the molecular wave function. [36,37] The inclusion of diffuse functions is often essential, [38] particularly when dealing with open-shell species like atomic oxygen or when modeling weakly bound intermediates and transition states. Diffuse functions extend the spatial flexibil-

ity of the basis set by introducing low-exponent Gaussian functions, improving the description of electron density in the outer regions of atoms and molecules. This refinement is crucial for accurately capturing charge distributions and long-range interactions. [39,40] However, the addition of diffuse functions significantly increases the computational cost, as the number of integrals grows due to the enhanced treatment of long-range electron interactions. Large basis sets increase the number of variational parameters in the wave function, leading to higher memory requirements and longer computation times. For large molecules or polymeric systems, this can pose convergence challenges, making some basis sets impractical for routine calculations. [38,41] To address the computational bottleneck associated with large basis sets, the Resolution of Identity (RI) approximation is often employed. [42] RI reduces the computational scaling of electron repulsion integrals by introducing an auxiliary basis set, effectively simplifying the four-center integrals into three-center terms. This approximation significantly speeds up calculations, particularly in DFT and post-HF methods, without substantially compromising accuracy. However, when large basis sets are used in conjunction with RI, convergence problems can arise due to the linear dependence of the auxiliary basis set. These issues become more pronounced as the basis set limit is approached, leading to numerical instabilities in wave function optimization. [43] This raises an important question: Is it always necessary to use highly diffuse basis sets to obtain reliable results, or can a judiciously chosen, more compact basis set provide a sufficient balance between accuracy and computational efficiency?

To address this, we evaluate different types of basis sets, both with and without diffuse functions, by assessing their performance in calculating the entrance barrier of an oxygen atom interacting with two small PAHs—naphthalene and phenanthrene—for which the use of diffuse functions is still affordable. [44,45]

2 Theoretical Methods

All the density functional theory (DFT) calculations were conducted using the ORCA [46] code with the ωB97X exchange-correlation functional [33,34] with Grimme's D3BJ dispersion correction. [47,48] Different types of basis sets were tested for this work, detailed as follows:

Pople's 6-311++G(3df,3pd) and 6-311G(3df,3pd) basis sets were used. [49–51] Pople's basis sets incorporate a triple-zeta split-valence representation, diffuse functions on both heavy atoms and hydrogen, and higher-order polarization functions (including three sets of d-functions and one set of f-functions for heavy atoms, as well as three sets of p-functions and one set of d-functions for hydrogen). Correlation-consistent polarized valence basis sets, such as cc-pVTZ and aug-cc-pVTZ, developed by Dunning and co-workers [52], are designed to accurately describe electron correlation and molecular properties. The cc-pVTZ basis set incorporates a triple-zeta representation for the valence orbitals, with three sets of functions for each orbital, along with polarization functions on heavy atoms to improve the description of bonding and electron distribution. The aug-cc-pVTZ basis set extends the cc-pVTZ set by adding diffuse functions on both

heavy atoms and hydrogen. Polarized correlation-consistent Gaussian basis sets, such as pcseg-2 and aug-pcseg-2, developed by Peterson and co-workers [53], are optimized for accurate DFT calculations. The pcseg-2 basis set incorporates a triple-zeta representation for the valence orbitals, along with polarization functions on heavy atoms to improve the description of bonding and electron distribution. The aug-pcseg-2 basis set extends the pcseg-2 set by including diffuse functions on both heavy atoms and hydrogen.

All calculations were performed using the resolution-of-identity (RI) method with an auto-generated auxiliary basis set. [54,55] They were optimized using a very tight self-consistent field (SCF) convergence criterion of 1×10^{-09} a.u. Minima were optimized using the Broyden–Fletcher–Goldfarb–Shanno (BFGS) method. [56] The minima were considered optimized when the maximum gradient was lower than 3×10^{-5} a.u. per Bohr radius. Transition states were optimized using an eigenvalue-following transition state-finding algorithm in ORCA and were considered optimized when the maximum gradient was less than 1×10^{-4} a.u. per Bohr radius. Harmonic vibrational frequencies were calculated to characterize local minima (no negative frequencies) and saddle points (one imaginary frequency only). The energies of the minima and transition states are all referenced to the reactants at infinite distance (naphthalene or phenanthrene and $O(^3P)$). All the electronic energies are corrected for the vibrational zero-point energy (ZPE).

3 Results

To evaluate the role of diffuse functions in the basis sets for the reaction of $O(^3P)$ with aromatic monomers, we report the potential energy surface for the entrance reaction of $O(^3P)$ with naphthalene and phenanthrene, as well as analyze the computational time required for each basis set.

3.1 $O(^3P)$+Naphthalene

The ωB97X-D functional [33,34], in conjunction with dispersion correction and the Pople basis sets has been shown in prior studies to adequately describe the reactivity of $O(^3P)$ with monocyclic aromatics such as benzene. [8,14] However, this approach is computationally expensive and may become impractical when modeling larger molecules such as naphthalene or phenanthrene.

Here, as shown in Fig. 2, we report results for the addition of an $O(^3P)$ to naphthalene to form the O-PAH adduct in the triplet spin state (the product). We tested the most commonly employed basis sets (e.g., cc-pVTZ and pcseg-2) and evaluated whether adding diffuse functions is necessary for modeling the attack of $O(^3P)$. Here, we employed ωB97X-D3BJ, as the older ωB97X-D is based on the earlier Grimme dispersion correction (D2), [57] whereas here we use the more accurate D3BJ in this work. [48]

To investigate the $O(^3P)$ addition onto naphthalene, we have selected the carbon of the C-H group located next to the inner carbons (which lack hydrogen),

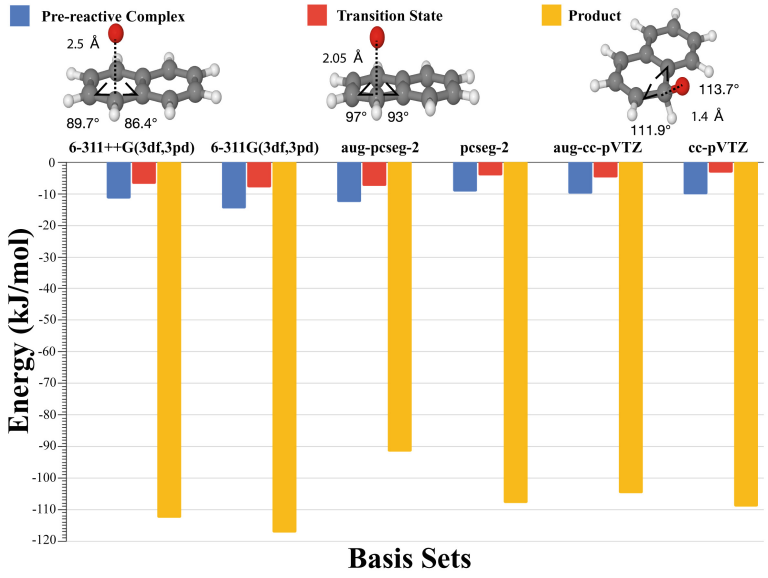

Fig. 2. Energy differences of the pre-reactive complex, transition state, and product, respectively, for different Basis Sets, relative to O(^{3}P) and naphthalene at infinite distance. The molecular structures of O(^{3}P) and naphthalene at the minima and saddle point are also reported including C-O distances and $C\widehat{-C-O}$ angles.

as previous studies [23,58] have shown that this position is particularly receptive to radical attachment (see Fig. 2). The addition of O(^{3}P) to naphthalene (Fig. 2) proceed with the formation of a weak pre-reactive complex, with a C-O distance of 2.54 Å, as shown in the first bar (blue color) for each basis set at ωB97X-D3BJ. The reaction then proceeds, at the same level of theory, by overcoming barriers, characterized by a partial bond formation and located at C-O distance of 2.05 Å, which are submerged considering the reactants at infinite distance (O+PAH). Once the barrier is passed, the product consists in the PAH-O adduct, with a C-O bond distance of 1.37 Å, as shown in the reaction depicted in Fig. 2.

Figure 2 shows the effect of diffuse functions when using different basis sets. The pre-reactive complex well ranges from −10 kJ/mol to −15 kJ/mol, with the removal of the diffuse functions leading to a slightly larger well, approximately 4 kJ/mol deeper, compared to the 6-311++G(3df,3pd) basis set. For the pcseg-2 series, we observe a different behavior: the pcseg-2 result yields a pre-reactive complex of −9 kJ/mol, which is lower than that of the aug-pcseg-2 basis set, which results in a well of about −13 kJ/mol. We did not find any differences for the cc-pVTZ basis set, where the presence of diffuse functions does not affect the pre-reactive complex, which remains at −10 kJ/mol. Overall, the Pople basis set overestimates the pre-reactive complex depth by a few kJ/mol compared to

the other basis sets. All the barrier results are submerged due to the presence of a favorable pre-reactive complex. These submerged barriers are reported in Table 2 and compared with literature values.

Table 1. Submerged barrier (E_{sub}) values, in kJ/mol, referenced to the pre-reactive complex, for the addition of O(^{3}P) to naphthalene (see PES in Fig. 2) computed at ωB97X-D3BJ using different basis sets in this work. These values are compared with literature (Lit.) data from theoretical studies conducted at BH&HLYP/6-31G(3d,3p)//B3LYP/6-311G(d,p) (Lit. [59]), M06-2X/cc-pVTZ//M06-2X/6-311G(d,p) (Lit. a [60]), M06-2X/6-311G(d,p) (Lit. b [60]) and CBS-QB3 (Lit. [23]).

Level of Theory	E_{sub}
6-311++G(3df,3pd)	4.83
6-311G(3df,3pd)	6.62
aug-pcseg-2	5.16
pcseg-2	5.12
aug-cc-pVTZ	5.10
cc-pVTZ	7.00
Lit. [59]	8.37
Lit. a [60]	4.25
Lit. b [60]	6.74

The submerged barrier values (Table 1) obtained with ωB97X-D3BJ are perfectly in line with those found in the literature at DFT level. [59,60] Regarding the barrier height, the effect of the diffuse function is such that 6-311++G(3df,3pd), in agreement with the values reported by Scapinello *et al.* [60] using the M06-2X/cc-pVTZ//M06-2X/6-311G(d,p) level of theory, underestimates the barrier height compared to when diffuse functions are included. The diffuse function in the pcseg-2 basis set does not impact the submerged barrier height, whereas the cc-pVTZ basis set results in a larger submerged barrier—similar to what is observed for the Pople-type basis sets—by about 2 kJ/mol. Overall, a 2 kJ/mol difference is small compared to the typical intrinsic errors of DFT functionals. [61] Therefore, for the barrier height and pre-reactive complex, diffuse functions do not have a major impact on the accuracy of the basis set within the uncertainty of the method. [61]

The reaction energy for product formation (Fig. 2) ranges from approximately −90 kJ/mol to -118 kJ/mol. Reported literature values are −92.27 kJ/mol at the M06-2X/6-311G(d,p) level of theory [60] and −93.3 kJ/mol at the BH&HLYP/6-31G(3d,3p)//B3LYP/6-311G(d,p) level. [59] Among the tested methods, only ωB97X-D3BJ/aug-pcseg-2 provides values in perfect agreement with the literature. In contrast, other basis sets overestimate the reaction energy for product formation by approximately 20 kJ/mol with respect to the literature values.

[59,60] The role of diffuse functions is more significant in the formation of the product, as indicated by differences larger than 2 kJ/mol between basis sets with and without diffuse functions (Fig. 2). Specifically, the 6-311++G(3df,3pd) and 6-311G(3df,3pd) basis sets yield values of −112 kJ/mol and −117 kJ/mol, respectively, resulting in a difference of 5 kJ/mol. Similarly, the aug-pcseg-2 and pcseg-2 basis sets predict values of −92 kJ/mol and −108 kJ/mol, respectively, with a difference of 16 kJ/mol. In contrast, the cc-pVTZ basis sets exhibit smaller discrepancies, yielding values of −105 kJ/mol and −109 kJ/mol, with a difference of only 4 kJ/mol.

The reported results in Fig. 2 are based on full optimization at each basis set type and include ZPE correction. To fully understand the observed discrepancies, we also report the values as single-point energies, without ZPE correction, using the ωB97X-D3BJ/6-311G(3df,3dp) geometry as a reference. This allows us to evaluate whether the observed discrepancies arise not only from the choice of basis set but also from the optimization of the geometry.

For the pre-reactive complex, the 6-311G(3df,3pd) basis set (Fig. 3) gives the lowest energy (−16.7 kJ/mol), while the highest value is obtained with pcseg-2 (−10.3 kJ/mol). The aug-pcseg-2 and aug-cc-pVTZ basis sets yield nearly identi-

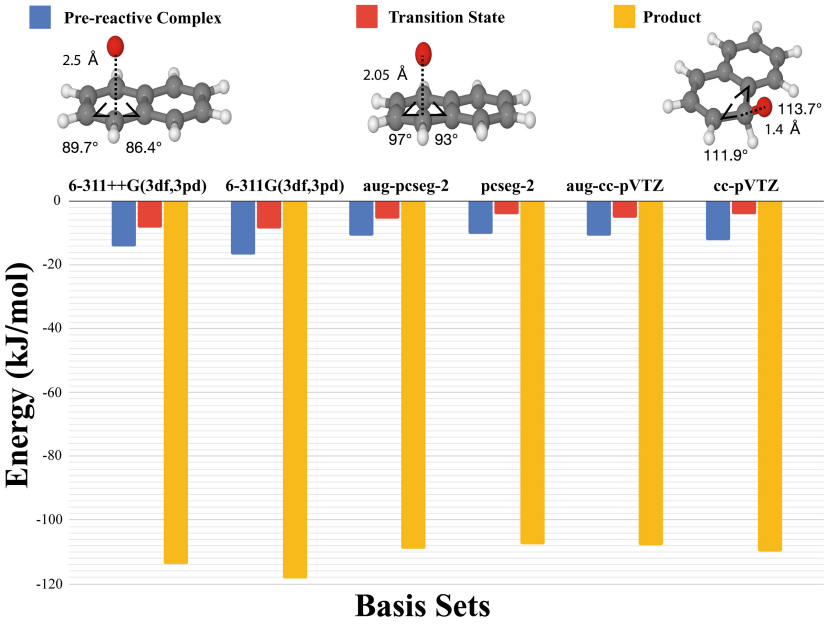

Fig. 3. Energy evaluation using the same geometry for all basis sets to study the energy differences due to the change of Basis Set types for the reaction of $O(^3P)$ with naphthalene. Those geometries are single-point energy evaluations, without ZPE correction, of the optimized geometries of the pre-reactive complex, transition state, and product at the ωB97X-D3BJ/6-311G(3df,3dp) level. The molecular structures of minima and saddle points are shown including C-O distances and $C\widehat{-C-O}$ angles.

cal values (−10.9 kJ/mol), suggesting that augmentation with diffuse functions has little impact on the energy at this stage of the reaction. The difference between 6-311G(3df,3pd) and 6-311++G(3df,3pd) (−16.7 vs. −14.2 kJ/mol) indicates a small effect of additional diffuse functions in this case.

At the transition state, all basis sets predict similar energies, ranging from −8.6 kJ/mol (6-311G(3df,3pd)) to −4.0 kJ/mol (cc-pVTZ). The pcseg-2 basis set gives a similar result (−4.1 kJ/mol), showing the highest value among the segment-contracted sets. The difference between the highest and lowest values is about 4.6 kJ/mol, which suggests that while basis set choice does influence the computed barrier height, the effect is less pronounced than in the pre-reactive complex or product.

For the product, the computed energies range from −107.5 kJ/mol (pcseg-2) to −118.2 kJ/mol (6-311G(3df,3pd)). The differences among the basis sets are more significant in this case, with a spread of approximately 10.7 kJ/mol. This variation suggests that the description of the electronic structure of the product is more sensitive to basis set choice than that of the transition state. Overall, while all basis sets capture the general trend of the reaction pathway, the computed energy differences depend on the choice of basis set. The largest differences are observed in the pre-reactive complex and the product, whereas the transition state energies remain relatively close across all methods. These variations highlight the impact of basis set selection on the computed reaction profile.

3.2 $O(^3P)$+Phenanthrene

To understand the size effect on the tested basis sets (see prior section), we computed the addition of $O(^3P)$ to phenanthrene (Fig. 4) using the same basis sets employed for naphthalene at the ωB97X-D3BJ level. The attack was conducted on the most reactive carbons as report by prior studies. [23,58] However, for the phenanthrene case, we could not include diffuse functions in the pcseg-2 and cc-pVTZ basis sets due to convergence problems caused by linear dependence in the basis, which arises when the basis set limit is reached, leading to convergence issues. Nevertheless, this is not a concern, as for naphthalene, we have observed that including diffuse functions in these basis sets does not significantly affect the results.

The results of the $O(^3P)$ reaction with phenanthrene are reported in Table 2. In the pre-reactive complex, the difference between the 6-311++G(3df,3pd) and the 6-311G(3df,3pd) basis set is 3 kJ/mol, while the difference between the pcseg-2 and cc-pVTZ basis sets is 1 kJ/mol. There are no significant differences between pcseg-2 and cc-pVTZ, whereas the inclusion of diffuse functions increases the energy of the pre-reactive complex by 4.5 kJ/mol for cc-pVTZ and 5.5 kJ/mol for pcseg-2 compared to 6-311++G(3df,3pd). The 6-311G(3df,3pd) basis set shows larger discrepancies, with a difference of 5.5 kJ/mol relative to pcseg-2 and 4.5 kJ/mol relative to cc-pVTZ.

For the transition state, all basis sets show a submerged barrier, except for cc-pVTZ, which is slightly emerged by 0.2 kJ/mol. The 6-311++G(3df,3pd) basis

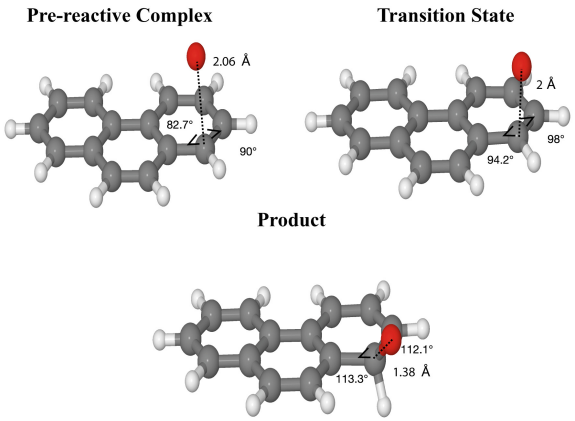

Fig. 4. Molecular structures, including C-O distances and $C\widehat{-C-O}$ angles, of the pre-reactive complex, transition states, and products of the O(^{3}P) + Phenanthrene reaction.

set agrees closely with pcseg-2, with a difference of 0.1 kJ/mol, while it diverges from 6-311G(3df,3pd) by 3.7 kJ/mol and by 1.1 kJ/mol relative to cc-pVTZ. The 6-311G(3df,3pd) basis set shows differences of 3.8 kJ/mol compared to pcseg-2 and 4.8 kJ/mol compared to cc-pVTZ. A difference of 1 kJ/mol is negligible compared to the error of the method. [61]

The phenanthrene-O (product), computed using the 6-311++G(3df,3pd) basis set, shows very small differences (Table 2) compared to pcseg-2 and cc-pVTZ, with deviations of 2.1 kJ/mol and 1.1 kJ/mol, respectively. The 6-311G(3df,3pd) basis set overestimates the reaction energy for product formation by approximately 7.2 kJ/mol compared to 6-311++G(3df,3pd), 9.3 kJ/mol compared to pcseg-2, and 8.3 kJ/mol compared to cc-pVTZ.

Overall, the phenanthrene results align with the trend observed for naphthalene.

Table 2. PES of the addition of O(^{3}P) to phenanthrene, showing energy differences with respect to the reactants at infinite distance (O(^{3}P) + phenanthrene). The reported energies, in kJ/mol, are calculated at the wB97-D3BJ level of theory and include ZPE correction.

	6-311++G(3df,3pd)	6-311G(3df,3pd)	pcseg-2	cc-pVTZ
Pre-reactive complex	−11.7	−14.7	−9.2	−10.2
TS	−0.9	−4.6	−0.8	0.2
Product	−99.4	−106.6	−97.3	−98.3

3.3 Computational Time

To evaluate the computational time of the selected basis set types (Fig. 5), we tested them for the case of naphthalene + O(^{3}P), considering both the computational time required and the number of self-consistent field (SCF) iterations needed to achieve convergence.

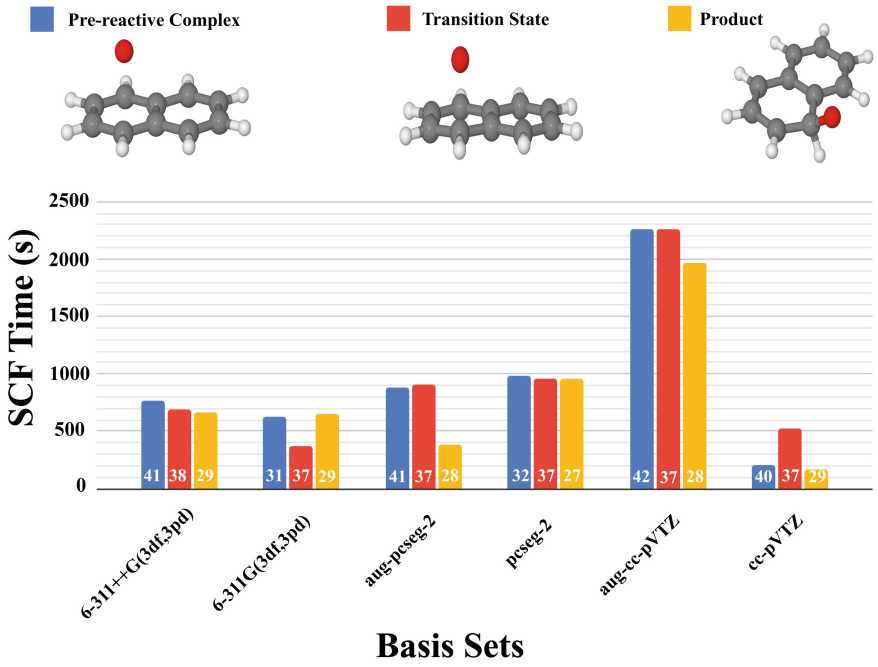

Fig. 5. SCF Time, for only one converged cycle, in seconds (s), for the reaction of O(^{3}P) to naphthalene in the pre-reactive complex, transition state, and product, using various basis sets, and reported in the same order for each basis set. The number of SCF cycles required to reach convergence is reported above each bar.

Examining the time to converge one SCF (Fig. 5), significant differences emerge among the basis sets. The computational cost varies considerably, with the largest times observed for the augmented correlation-consistent basis set (aug-cc-pVTZ). Specifically, for the pre-reactive complex and transition state (TS), this basis set results in the highest SCF times, 2255 s and 2267 s, respectively. The second most time-consuming basis set is pcseg-2, which consistently requires nearly 950–990 s across all species. On the other hand, the cc-pVTZ basis set displays the lowest computational times, particularly for the product, where the SCF time is only 169 s. Similarly, 6-311++G(3df,3pd) and 6-311G(3df,3pd) show moderate computational costs, with times generally below 800 s. Despite variations in computational time, the number of SCF iterations required to achieve convergence remains relatively consistent across basis sets.

The transition state (TS) exhibits a nearly uniform behavior, requiring 37 iterations in all cases except for 6-311++G(3df,3pd), which converges in 38 iterations. The pre-reactive complex generally demands a higher number of iterations, with the aug-cc-pVTZ basis set reaching the highest count at 42 iterations, while the pcseg-2 and 6-311G(3df,3pd) basis sets require slightly fewer iterations (32 and 31, respectively). For the product, a slightly lower number of iterations is observed, ranging from 27 (pcseg-2) to 29 (most other basis sets). These results suggest that computational time does not directly correlate with the number of SCF iterations. For instance, aug-cc-pVTZ and pcseg-2 require more time despite having iteration counts comparable to other basis sets. This discrepancy can be attributed to the intrinsic complexity and size of the basis sets, which increase the computational burden per iteration. Augmented basis sets such as aug-cc-pVTZ include diffuse functions, which can lead to more complex integral evaluations and slower matrix operations, explaining the extended SCF times. Similarly, the segmented-contracted pcseg-2 basis set may involve additional computational overhead despite converging in fewer iterations than aug-cc-pVTZ. Conversely, cc-pVTZ, which is a non-augmented correlation-consistent basis set, exhibits the shortest SCF times across all cases while maintaining iteration counts comparable to other basis sets. This highlights its computational efficiency, making it an attractive choice when balancing accuracy and cost. Overall, the results underscore the trade-off between basis set complexity and computational expense. While larger basis sets offer improved accuracy, they also come with significant computational costs, which must be carefully considered when modeling large systems.

4 Conclusions

Modeling the O(^{3}P) reaction with large aromatic compounds, such as naphthalene and phenanthrene, as well as polymers, to study the degradation of these materials in space requires a careful selection of basis sets that balance efficiency and computational cost. In this work, we tested several basis sets with and without diffuse functions (6-311++G(3df,3pd), 6-311G(3df,3pd), aug-pcseg-2, pcseg-2, aug-cc-pVTZ, and cc-pVTZ) at the ωB97X-D3BJ DFT level.

We found that the addition of diffuse functions for the reaction of O(^{3}P) with naphthalene and phenanthrene does not significantly affect the performance of the basis sets in terms of energy pathways, although it increases the computational burden. For the addition of O(^{3}P) to phenanthrene, the use of diffuse functions in pcseg-2 and cc-pVTZ is prohibitive due to linear dependence of the basis set as it reaches the basis set limit.

Overall, cc-pVTZ achieved the lowest computational cost while maintaining accuracy comparable to basis sets that include diffuse functions, such as 6-311++G(3df,3pd), for both naphthalene and phenanthrene cases. It is also important to note that basis set superposition error (BSSE) was not explicitly addressed, as triple-zeta basis sets generally lead to BSSE values smaller than the typical errors associated with DFT functionals. Moreover, theoretical studies by Mentel *et al.* [62] indicates that applying counterpoise corrections can

sometimes introduce new imbalances, rather than improve agreement with basis set limit results. To avoid this potential source of bias—particularly when comparing the influence of diffuse functions across different basis sets—counterpoise corrections were not employed. Additionally, we did not adopt a computational strategy involving geometry optimization with triple-zeta basis sets followed by single-point calculations using their augmented counterparts. Although this approach can lower computational cost, our results show that the presence of diffuse functions has minimal impact on the potential energy surface (PES). Finally, to ensure consistency and allow for fair comparisons, all calculations were performed on the same computer node, using identical CPU and memory configurations when measuring the SCF time.

The present results show that the inclusion of diffuse functions is not always necessary and requires careful consideration, as in the case of neutral PAHs, where it does not affect accuracy but increases computational cost. The latter could be prohibitive when modeling $O(^3P)$ reactions with large monomers and/or polymers to evaluate the efficiency of these materials in satellite applications in LEO and LMO environments.

Acknowledgments. D.C. acknowledges the CINECA award under the ISCRA initiative, for the availability of high performance computing resources and support. We acknowledge financial support under the National Recovery and Resilience Plan (NRRP),Mission 4, Component 2, Investment 1.1, Call for tender No. 1409 published on 14.09.2022 by the Italian Ministry of University and Research (MUR), funded by the European Union – NextGenerationEU – Project Title P20223H8CK Degradation of space-technology polymers by thermospheric oxygen atoms and ions: an exploration of the reaction mechanisms at an atomistic level (ThermOPoly) – CUP J53D23014440001 – Grant Assignment Decree No. 1386 adopted on 01.09.2023 by the Italian Ministry of University and Research (MUR). We acknowledges COLONIZE project from the University of Perugia: indagini preliminari su risposte biologiche, materiali cementizi alternativi e nuove fonti energetiche per affrontare la colonizzazione infrastrutturale dello Spazio.

Disclosure of Interests. The authors have no competing interests to declare that are relevant to the content of this article.

References

1. Grossman, E., Gouzman, I.: Space environment effects on polymers in low earth orbit. Nucl. Instrum. Methods Phys. Res. B **208**, 48–57 (2003). https://doi.org/10.1016/S0168-583X(03)00640-2
2. Strganac, T.W., Letton, A., Rock, N.I., Williams, K.D., Farrow, D.A.: Characterization of polymer films retrieved from Nasa's long duration exposure facility. J. Spacecr. Rockets **32**(3), 502–506 (1995). https://doi.org/10.2514/3.26643
3. Groh, K., Banks, B.A., Mccarthy, C.E., Rucker, R.N., Roberts, L.M., Berger, L.A.: Misse 2 peace polymers atomic oxygen erosion experiment on the international space station. High Perform. Polym. **20**(4–5), 388–409 (2008). https://doi.org/10.1177/0954008308089705

4. Minton, T.K., et al.: Atomic oxygen effects on POSS polyimides in low earth orbit. ACS Appl. Mater. Interfaces. **4**(2), 492–502 (2012). https://doi.org/10.1021/am201509n
5. Rahnamoun, A., van Duin, A.: Reactive molecular dynamics simulation on the disintegration of Kapton, POSS polyimide, amorphous silica, and Teflon during atomic oxygen impact using the ReaxFF reactive force-field method. J. Phys. Chem. A **118**(15), 2780–2787 (2014). https://doi.org/10.1021/jp4121029
6. Zhang, Y., et al.: The effects of atomic oxygen and ion irradiation degradation on multi-polymers: a combined ground-based exposure and ReaxFF-MD simulation. Polym. Degrad. Stab. **205**, 110134 (2022). https://doi.org/10.1016/j.polymdegradstab.2022.110134
7. Zeng, F., Peng, C., Liu, Y., Qu, J.: Reactive molecular dynamics simulations on the disintegration of PVDF, FP-POSS, and their composite during atomic oxygen impact. J. Phys. Chem. A **119**(30), 8359–8368 (2015). https://doi.org/10.1021/acs.jpca.5b03783
8. Cavallotti, C., et al.: Theoretical study of the extent of intersystem crossing in the $O(^3P) + C_6H_6$ reaction with experimental validation. J. Phys. Chem. Lett. **11**(22), 9621–9628 (2020). https://doi.org/10.1021/acs.jpclett.0c02866
9. Cavallotti, C., et al.: Crossed-beam and theoretical studies of multichannel nonadiabatic reactions: branching fractions and role of intersystem crossing for $O(^3P)$ + 1,3-butadiene. Faraday Discuss. **238**, 161–182 (2022). https://doi.org/10.1039/D2FD00037G
10. Gimondi, I., Cavallotti, C., Vanuzzo, G., Balucani, N., Casavecchia, P.: Reaction dynamics of $O(^3P)$ + propyne: II. primary products, branching ratios, and role of intersystem crossing from Ab initio coupled triplet/singlet potential energy surfaces and statistical calculations. J. Phys. Chem. A **120**(27), 4619–4633 (2016). https://doi.org/10.1021/acs.jpca.6b01564
11. Leonori, F., et al.: Experimental and theoretical studies on the dynamics of the $O(^3P)$ + propene reaction: primary products, branching ratios, and role of intersystem crossing. J. Phys. Chem. C **119**(26), 14632–14652 (2015). https://doi.org/10.1021/jp512670y
12. Fu, B., et al.: Intersystem crossing and dynamics in $O(^3P) + C_2H_4$ multichannel reaction: experiment validates theory. Proc. Natl. Acad. Sci. U.S.A. **109**(25), 9733–9738 (2012). https://doi.org/10.1073/pnas.1202672109
13. Recio, P., et al.: Intersystem crossing in the entrance channel of the reaction of $O(^3P)$ with pyridine. Nat. Chem. **14**(12), 1405–1412 (2022). https://doi.org/10.1038/s41557-022-01047-3
14. Vanuzzo, G., et al.: Crossed-beam and theoretical studies of the $O(^3P, {}^1D)$ + benzene reactions: primary products, branching fractions, and role of intersystem crossing. J. Phys. Chem. A **125**(38), 8434–8453 (2021). https://doi.org/10.1021/acs.jpca.1c06913
15. Ramasesha, K., Savee, J.D., Zádor, J., Osborn, D.L.: A new pathway for intersystem crossing: unexpected products in the $O(^3P)$ + cyclopentene reaction. J. Phys. Chem. A **125**(45), 9785–9801 (2021). https://doi.org/10.1021/acs.jpca.1c05817
16. Liang, P., et al.: Reactions $O(^3P, {}^1D)$ + HCCCN($X^1\,\Sigma^+$) (cyanoacetylene): crossed-beam and theoretical studies and implications for the chemistry of extraterrestrial environments. J. Phys. Chem. A **127**(3), 685–703 (2023). https://doi.org/10.1021/acs.jpca.2c07708
17. Balucani, N., et al.: Crossed molecular beam experiments and theoretical simulations on the multichannel reaction of toluene with atomic oxygen. Faraday Discuss. **251**, 523–549 (2024). https://doi.org/10.1039/D3FD00181D

18. Piergiorgio Casavecchia, F.L., Balucani, N.: Reaction dynamics of oxygen atoms with unsaturated hydrocarbons from crossed molecular beam studies: primary products, branching ratios and role of intersystem crossing. Int. Rev. Phys. Chem. **34**(2), 161–204 (2015). https://doi.org/10.1080/0144235X.2015.1039293
19. Balucani, N., Leonori, F., Casavecchia, P., Fu, B., Bowman, J.M.: Crossed molecular beams and Quasiclassical trajectory surface hopping studies of the multichannel nonadiabatic O(^{3}P) + ethylene reaction at high collision energy. J. Phys. Chem. A **119**(50), 12498–12511 (2015). https://doi.org/10.1021/acs.jpca.5b07979
20. Rosi, M., Balucani, N., Casavecchia, P., Mancini, L., Pannacci, G., Vanuzzo, G.: A computational strategy for the theoretical investigation of the reactions between atomic oxygen and aromatic compounds. In: Computational Science and Its Applications – ICCSA 2024 Workshops, vol. 14818, pp. 71–83 (2024).https://doi.org/10.1007/978-3-031-65273-8_5
21. Catlow, R., Burke, P., Goodfellow, J., Tildesley, D., Wilson, M., Morokuma, K.: New challenges in quantum chemistry: quests for accurate calculations for large molecular systems. Philos. Trans. R. Soc. A **360**(1795), 1149–1164 (2002). https://doi.org/10.1098/rsta.2002.0993
22. Campisi, D.: Interstellar catalysts and the PAH universe. Scolarly Publications Leiden University (2021). https://hdl.handle.net/1887/3210124
23. Kayanuma, M., Suzuki, S., Choe, Y.K., Shimoi, Y.: Structure dependency of the reactivity of aromatic hydrocarbons involving the formation of oxygenated polycyclic aromatic hydrocarbons (OPAHs). Chem. Phys. Lett. **754**, 137652 (2020). https://doi.org/10.1016/j.cplett.2020.137652
24. Frerichs, H., Tappe, M., Wagner, H.G.: Comparison of the reactions of mono- and polycyclic aromatic hydrocarbons with oxygen atoms. Ber. Bunsenges. Phys. Chem. **94**(11), 1404–1407 (1990). https://doi.org/10.1002/bbpc.199000043
25. Campisi, D., et al.: Superhydrogenation of pentacene: the reactivity of zigzag-edges. Phys. Chem. Chem. Phys. **22**, 1557–1565 (2020). https://doi.org/10.1039/C9CP05440E
26. Campisi, D., Candian, A.: Do defects in PAHs promote catalytic activity in space? stone-wales pyrene as a test case. Phys. Chem. Chem. Phys. **22**, 6738–6748 (2020). https://doi.org/10.1039/C9CP06523G
27. Campisi, D., Lamberts, T., Dzade, N.Y., Martinazzo, R., ten Kate, I.L., Tielens, A.: Interaction of aromatic molecules with forsterite: accuracy of the periodic DFT-D4 method. J. Phys. Chem. A **125**(13), 2770–2781 (2021). https://doi.org/10.1021/acs.jpca.1c02326
28. Campisi, D., Tielens, A., Dononelli, W.: The role of point defect reconstructions and polycyclic aromatic hydrocarbons in silicate dust preservation. Mon. Not. R. Astron. Soc. **533**(2), 2282–2293 (2024). https://doi.org/10.1093/mnras/stae1962
29. Campisi, D., Lamberts, T., Dzade, N.Y., Martinazzo, R., ten Kate, I.L., Tielens, A.: Adsorption of polycyclic aromatic hydrocarbons and C_{60} onto forsterite: C-H bond activation by the Schottky vacancy. ACS Earth Space Chem. **6**(8), 2009–2023 (2022). https://doi.org/10.1021/acsearthspacechem.2c00084
30. McCabe, M.N., et al.: Formation of phenylacetylene and benzocyclobutadiene in the ortho-benzyne + acetylene reaction. Phys. Chem. Chem. Phys. **24**, 1869–1876 (2022). https://doi.org/10.1039/D1CP05183K
31. Tielens, A.: Interstellar polycyclic aromatic hydrocarbon molecules. Annu. Rev. Astron. Astrophys. **46**, 289–337 (2008). https://doi.org/10.1146/annurev.astro.46.060407.145211
32. Parr, R.G.: Density functional theory. Annu. Rev. Phys. Chem. **34**, 631–656 (1983). https://doi.org/10.1146/annurev.pc.34.100183.003215

33. Chai, J.D., Head-Gordon, M.: Systematic optimization of long-range corrected hybrid density functionals. J. Chem. Phys. **128**(8), 084106 (2008). https://doi.org/10.1063/1.2834918
34. Chai, J.D., Head-Gordon, M.: Long-range corrected hybrid density functionals with damped atom-atom dispersion corrections. Phys. Chem. Chem. Phys. **10**, 6615–6620 (2008). https://doi.org/10.1039/B810189B
35. Caracciolo, A., Vanuzzo, G., Balucani, N., Stranges, D., Cavallotti, C., Casavecchia, P.: Observation of H displacement and H_2 elimination channels in the reaction of $O(^3P)$ with 1-butene from crossed beams and theoretical studies. Chem. Phys. Lett. **683**, 105–111 (2017). https://doi.org/10.1016/j.cplett.2017.02.036
36. Ahlrichs, R., Taylor, P.R.: The choice of gaussian basis sets for molecular electronic structure calculations. J. Chim. Phys. **78**, 315–324 (1981). https://doi.org/10.1051/jcp/1981780315
37. Schuchardt, K.L., et al.: Basis set exchange: a community database for computational sciences. J. Chem. Inf. Model. **47**(3), 1045–1052 (2007). https://doi.org/10.1021/ci600510j
38. Lynch, B.J., Zhao, Y., Truhlar, D.G.: Effectiveness of diffuse basis functions for calculating relative energies by density functional theory. J. Phys. Chem. A **107**(9), 1384–1388 (2003). https://doi.org/10.1021/jp021590l
39. Jensen, F.: Polarization consistent basis sets. III. the importance of diffuse functions. J. Chem. Phys. **117**(20), 9234–9240 (2002). https://doi.org/10.1063/1.1515484
40. Papajak, E., Zheng, J., Xu, X., Leverentz, H.R., Truhlar, D.G.: Perspectives on basis sets beautiful: seasonal plantings of diffuse basis functions. J. Chem. Theory Comput. **7**(10), 3027–3034 (2011). https://doi.org/10.1021/ct200106a
41. Papajak, E., Truhlar, D.G.: Efficient diffuse basis sets for density functional theory. J. Chem. Theory Comput. **6**(3), 597–601 (2010). https://doi.org/10.1021/ct900566x
42. Skylaris, C.K., Gagliardi, L., Handy, N., Ioannou, A., Spencer, S., Willetts, A.: On the resolution of identity coulomb energy approximation in density functional theory. J. Mol. Struct. THEOCHEM **501–502**, 229–239 (2000). https://doi.org/10.1016/S0166-1280(99)00434-0
43. Pedersen, T.B., Aquilante, F., Lindh, R.: Density fitting with auxiliary basis sets from Cholesky decompositions. Theor. Chem. Acc. **124**(1), 1–10 (2009). https://doi.org/10.1007/s00214-009-0608-y
44. Qu, X.W., Zuo, P.P., Li, Y.M., Li, N., Shen, W.Z.: Mechanism for the catalytic thermal polycondensation of naphthalene at low temperature. J. Fuel Chem. Technol. **50**(10), 1259–1270 (2022). https://doi.org/10.1016/S1872-5813(22)60021-5
45. Hanemann, T., Böhm, J., Honnef, K., Ritzhaupt-Kleissl, E., HauSSelt, J.: Polymer/phenanthrene-derivative host-guest systems: rheological, optical and thermal properties. Macromol. Mater. Eng. **292**(3), 285–294 (2007). https://doi.org/10.1002/mame.200600409
46. Neese, F., Wennmohs, F., Becker, U., Riplinger, C.: The ORCA quantum chemistry program package. J. Chem. Phys. **152**(22), 224108 (2020). https://doi.org/10.1063/5.0004608
47. Grimme, S., Antony, J., Ehrlich, S., Krieg, H.: A consistent and accurate ab initio parametrization of density functional dispersion correction (DFT-D) for the 94 elements H-Pu. J. Chem. Phys. **132**(15), 154104 (2010). https://doi.org/10.1063/1.3382344

48. Grimme, S., Ehrlich, S., Goerigk, L.: Effect of the damping function in dispersion corrected density functional theory. J. Comput. Chem. **32**(7), 1456–1465 (2011). https://doi.org/10.1002/jcc.21759
49. Krishnan, R., Binkley, J.S., Seeger, R., Pople, J.A.: Self-consistent molecular orbital methods. XX. a basis set for correlated wave functions. J. Chem. Phys. **72**(1), 650–654 (1980). https://doi.org/10.1063/1.438955
50. McLean, A.D., Chandler, G.S.: Contracted gaussian basis sets for molecular calculations. I. second row atoms, Z=11-18. J. Chem. Phys. **72**(10), 5639–5648 (1980). https://doi.org/10.1063/1.438980
51. Frisch, M.J., Pople, J.A., Binkley, J.S.: Self-consistent molecular orbital methods 25. supplementary functions for gaussian basis sets. J. Chem. Phys. **80**(7), 3265–3269 (1984). https://doi.org/10.1063/1.447079
52. Dunning, T.: Gaussian basis sets for use in correlated molecular calculations. I. The atoms boron through neon and hydrogen. J. Chem. Phys. **90**(2), 1007–1023 (1989). https://doi.org/10.1063/1.456153
53. Jensen, F.: Unifying general and segmented contracted basis sets. segmented polarization consistent basis sets. J. Chem. Theory Comput. **10**(3), 1074–1085 (2014). https://doi.org/10.1021/ct401026a
54. Neese, F.: An improvement of the resolution of the identity approximation for the formation of the coulomb matrix. J. Comput. Chem. **24**(14), 1740–1747 (2003). https://doi.org/10.1002/jcc.10318
55. Stoychev, G.L., Auer, A.A., Neese, F.: Automatic generation of auxiliary basis sets. J. Chem. Theory Comput. **13**(2), 554–562 (2017). https://doi.org/10.1021/acs.jctc.6b01041
56. Head, J.D., Zerner, M.C.: A Broyden–Fletcher–Goldfarb–Shanno optimization procedure for molecular geometries. Chem. Phys. Lett. **122**(3), 264–270 (1985). https://doi.org/10.1016/0009-2614(85)80574-1
57. Grimme, S.: Accurate description of van der Waals complexes by density functional theory including empirical corrections. J. Comput. Chem. **25**(12), 1463–1473 (2004). https://doi.org/10.1002/jcc.20078
58. Santos, R.C., Agapito, F., Gonçalves, E.M., Martinho Simões, J.A., Borges dos Santos, R.M.: Energetics of H-atom addition to naphthalene: a thermochemical cycle from tetralin to naphthalene. J. Chem. Thermodyn. **61**, 83–89 (2013). https://doi.org/10.1016/j.jct.2013.01.028
59. Orrego, J.F., Truong, T.N., Mondragón, F.: A linear energy relationship between activation energy and absolute hardness: a case study with the O(^{3}P) atom-addition reactions to polyaromatic hydrocarbons. J. Phys. Chem. A **112**(36), 8205–8207 (2008). https://doi.org/10.1021/jp805012f
60. Scapinello, M., Martini, L.M., Tosi, P., Maranzana, A., Tonachini, G.: Molecular growth of PAH-like systems induced by oxygen species: experimental and theoretical study of the reaction of naphthalene with HO ($^2\Pi_{3/2}$), O(^{3}P), and O_2($^3\Sigma_g^-$). RSC Adv. **5**, 38581–38590 (2015). https://doi.org/10.1039/C5RA05129K
61. Mardirossian, N., Head-Gordon, M.: How accurate are the Minnesota density functionals for noncovalent interactions, isomerization energies, thermochemistry, and barrier heights involving molecules composed of main-group elements? J. Chem. Theory Comput. **12**(9), 4303–4325 (2016). https://doi.org/10.1021/acs.jctc.6b00637
62. Mentel, M., Baerends, E.J.: Can the counterpoise correction for basis set superposition effect be justified? J. Chem. Theory Comput. **10**(1), 252–267 (2014). https://doi.org/10.1021/ct400990u